

Hydrolysis of insulin chain B using zirconium(IV) at neutral pH[†]

Sarah S. Cepeda and Kathryn B. Grant*

Received (in Gainesville, FL, USA) 11th October 2007, Accepted 5th February 2008

First published as an Advance Article on the web 14th February 2008

DOI: 10.1039/b715589a

Zirconium(IV) hydrolyzes the 30-mer oligopeptide oxidized bovine insulin chain B after 4 h to 8 h of treatment at ~pH 7.0 and 60 °C: MALDI-TOF and HPLC-ESI-MS and MS/MS data show significant levels of cleavage at Gly8-Ser9, Gly20-Glu21, Ser9-His10, Cys(SO₃H)7-Gly8, and Cys(SO₃H)19-Gly20 amide bonds within the oligopeptide.

There has been widespread interest in the development of metal complexes that hydrolyze peptide amide bonds under mild conditions of pH and temperature.¹ These compounds are of great importance due to their potential applications in the analysis of protein solution structure, in protein engineering, and in therapeutics.^{1d,f,h,2} Our own research efforts have primarily focused on zirconium(IV). Because of its enhanced Lewis acid strength, oxophilicity,³ tendency to form complexes with high coordination numbers,³ and rapid ligand-exchange kinetics,⁴ this metal center should be able to catalyze peptide hydrolysis by activating an amide carbonyl carbon in the peptide backbone while delivering a hydroxide nucleophile to the scissile amide bond.^{1f} Recent efforts in our laboratory have demonstrated that Zr^{IV} in the presence of 4,13-diaza-18-crown-6 has excellent reactivity: *t*_{1/2} values are 5.3 ± 0.1 h and 36.6 ± 2.7 h for Zr^{IV}-assisted hydrolysis of the dipeptide Gly-Glu at pH 7.1/60 °C and at pH 7.3/37 °C.^{1f} (These half-lives represent significant rate enhancements compared to the *t*_{1/2} of ~250 years for spontaneous hydrolysis of unactivated peptide amide bonds at pH 7.0 and 37 °C).⁵ The formation of insoluble Zr^{IV} precipitates during the cleavage reactions led us to speculate that hydrolysis of peptides by Zr^{IV}/4,13-diaza-18-crown-6 might have a heterogeneous component similar to peptide hydrolysis by lanthanide hydroxide gels.⁶ Yet, in spite of the attributes of Zr^{IV}, the largest peptide to have been hydrolyzed by this metal center was Ala-Gly-Asp-Val.^{1f} To address this size limitation, herein we report efficient, Zr^{IV}-assisted hydrolysis of the 30-mer oligopeptide oxidized bovine insulin chain B.

In a typical cleavage reaction, 500 μM to 1 mM of oxidized bovine insulin chain B was added to 20 mM of 4,13-diaza-18-crown-6⁷ in the presence or absence of 10 mM of ZrCl₄. Hydrolysis reactions were allowed to proceed at pH 6.9–7.2 and 60 °C. Aliquots were removed at ~*t* = 0 h, 4 h, and 8 h

time points, quenched with the strong chelating agent EDTA, and then analyzed by HPLC-electrospray ionization mass spectrometry (ESI-MS) or by matrix-assisted laser desorption ionization time-of-flight (MALDI-TOF) MS. Mass spectral peak assignments of peptide hydrolysis products were made using FindPept software and ESI tandem mass spectrometry (MS/MS) (Fig. 1a and 1b; Tables S1 and S2 in ESI). Each of the peptide fragments produced by Zr^{IV}/4,13-diaza-18-crown-6 was defined as either an apparent major, intermediate, or trace product depending on its percent relative abundance in the HPLC-ESI chromatograms and MALDI-TOF mass spectra. In Fig. 1c is the primary amino acid sequence of insulin chain B showing the positions of peptide amide bond hydrolysis indicated by the MS data. In addition to percent relative abundance, Tables S1 and S2 summarize observed *vs.* calculated *m/z* values.

The HPLC-ESI chromatograms and MALDI-TOF mass spectra in Fig. 2 and Fig. 3 reveal the time-dependent appearance of prominent insulin chain B peptide hydrolysis products B, C, D, E, F, G, I, K, K⁺, L, W, and X. It is evident that shorter peptide fragments B, D, F, I, K, K⁺, L, W, and X become more dominant as the reaction proceeds from *t* = 4 h to *t* = 8 h, while the larger fragments C, E, G are prominent only at *t* = 4 h (Fig. 2).

The cleavage yields corresponding to the HPLC-ESI chromatograms shown in Fig. 2 were estimated by taking the sum of the peak areas of all the peptide hydrolysis products, dividing this sum by the total peak areas of the peptide hydrolysis products added to the peak area of any remaining unhydrolyzed peptide, and then multiplying the quotient by 100: hydrolysis yield = [sum of all peptide hydrolysis product peak areas/(sum of all peptide hydrolysis product peak areas + unhydrolyzed insulin chain B peak area)] × 100. In the presence of Zr^{IV}/4,13-diaza-18-crown-6, these values were 0% at *t* = 0 h, 15% at *t* = 4 h and 51% at *t* = 8 h (pH 7.0 and 60 °C). In parallel control reactions in which ZrCl₄ was substituted by equivalent volumes of water, corresponding values were minimal (0% at *t* = 0 h, 0% at *t* = 4 h and 3% at *t* = 8 h).

As expected, a larger number of peptide fragments was detected by HPLC-ESI-MS in comparison to MALDI-TOF MS. (In complex mixtures of analytes, competition for charge can lead to ion suppression. As a result, pre-separation is often needed to enhance sensitivity).⁸ Notwithstanding, the MALDI and HPLC-ESI experiments are in good general agreement (Fig. 1–3). The data collectively indicate that Zr^{IV}/4,13-diaza-18-crown-6 produces major amounts of hydrolysis at the following five amide bonds: Gly8-Ser9, Gly20-Glu21, Ser9-His10, Cys(SO₃H)7-Gly8, and Cys(SO₃H)19-Gly20.

Department of Chemistry, Center for Biotechnology and Drug Design, Georgia State University, P.O. Box 4098, Atlanta, GA 30302-4098, USA. E-mail: kbgrant@gsu.edu; Fax: +1-404-413-5505; Tel: +1-404-413-5522

[†] Electronic supplementary information (ESI) available: Details concerning general experimental materials; HPLC-ESI and MALDI-TOF MS data; Zr^{IV}-assisted lactamization and deamidation reactions. See DOI: 10.1039/b715589a

(a) Peptides Observed in ESI Mass Spectra: (A: Phe1 to Ala30)

Major, Int., and Trace HPLC Products:

B:	Phe1 to Cys(SO ₃ H) 7
B†:	Phe1 to Cys(SO ₃ H) 7
C:	Gly8 to Ala30
D:	Phe1 to Gly8
D†:	Phe1 to Gly8
E:	Ser9 to Ala30
F:	Phe1 to Ser9
F†:	Phe1 to Ser9
G:	His10 to Ala30

Major, Int., and Trace HPLC Products:

H:	Phe1 to Cys(SO ₃ H) 19
I:	Gly20 to Ala30
J:	Phe1 to Gly20
K:	Glu21 to Ala30
K†:	pyroGlu21 to Ala30
L:	Phe1 to Leu6
M:	Leu6 to Tyr16

Int. and Trace HPLC Products:

N:	Gly8 to Cys(SO ₃ H) 19
O:	Gly8 to Gly20
P:	Ser9 to Cys(SO ₃ H) 19
Q:	Ser9 to Gly20
R:	His10 to Cys(SO ₃ H) 19
S:	His10 to Gly20
T:	His10 to Lys29
U:	Val12 to Ala30
V:	Leu11 to Ala30
W:	Gly23 to Ala30
X:	Phe24 to Ala30

(b) Peptides Observed in MALDI-TOF Mass Spectra: (A: Phe1 to Ala30)

Major MS Products: E, K†

E:	Ser9 to Ala30
K†:	pyroGlu21 to Ala30

Int. MS Products: C, G, I

C:	Gly8 to Ala30
G:	His10 to Ala30
I:	Gly20 to Ala30

Trace MS Products: M, T, U, V

M:	Leu6 to Tyr16
T:	His10 to Lys29
U:	Val12 to Ala30
V:	Leu11 to Ala30

(c) Insulin Chain B Cleavage Pattern:

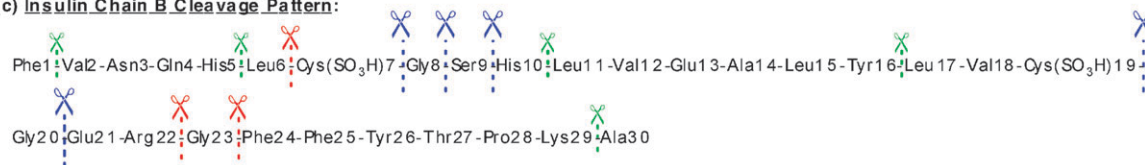


Fig. 1 Peptides detected in (a) HPLC-ESI and (b) MALDI-TOF mass spectra. The colors blue, red, and green identify apparent major, intermediate, and trace hydrolysis products, respectively. “†” = deamidation of Asn3 to Asp3, and/or Gln4 to Glu4. “†” = lactamization of Glu21 to pyroglutamate21 (pyroGlu21). (c) Corresponding Zr^{IV}/4,13-diaza-18-crown-6 cleavage sites superimposed on the amino acid sequence of oxidized bovine insulin chain B.

With respect to Gly8-Ser9, cleavage of Xaa-Ser(Thr) in peptides and proteins containing the sequence Xaa-Ser(Thr)-His has been extensively documented for Cu^{II},^{2b,9a,b,e,f} Ni^{II},^{1b} and Pd^{II},^{9b-d} and is thought to involve an N → O acyl rearrange-

ment promoted by the hydroxyl group side chains of serine or threonine.^{1b,9a,d} We also expected to observe significant levels of hydrolysis at Gly20-Glu21 and at Ser9-His10. In a previously published report, we demonstrated that Zr^{IV}/4,13-diaza-18-crown-6 displays a clear preference for hydrolysis of neutral and negatively charged peptides containing glycine or amino acids with oxygen-rich side chains.^{1f} (In fact,

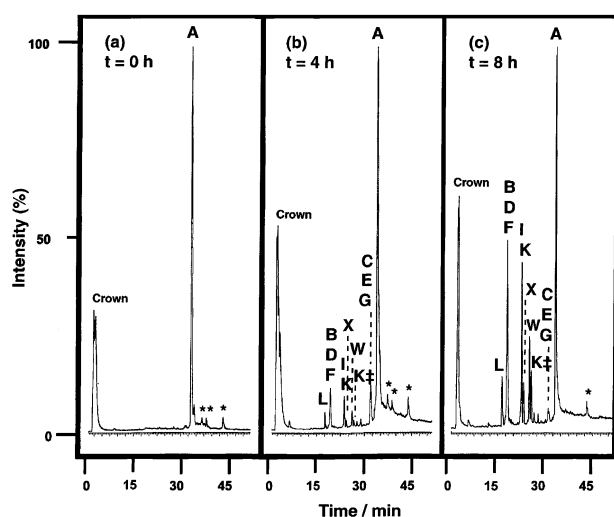


Fig. 2 HPLC chromatograms of 500 μM of insulin chain B treated with 10 mM ZrCl₄ in 20 mM 4,13-diaza-18-crown-6 for *t* = (a) 0 h, (b) 4 h, and (c) 8 h (pH 7.0 and 60 °C). Peak A is unhydrolyzed insulin chain B. Peaks B, D, F, I, K, and peaks L, X, W, K†, C, E, G correspond to apparent major and intermediate peptide hydrolysis products, respectively. Trace hydrolysis products are in Table S1 (in ESI). Representative ESI mass spectra are in Fig. S1 to S3. “Crown” identifies the azacrown ether. “*” identifies Na-adducted monomer and Na-adducted cluster dimers of peak A.

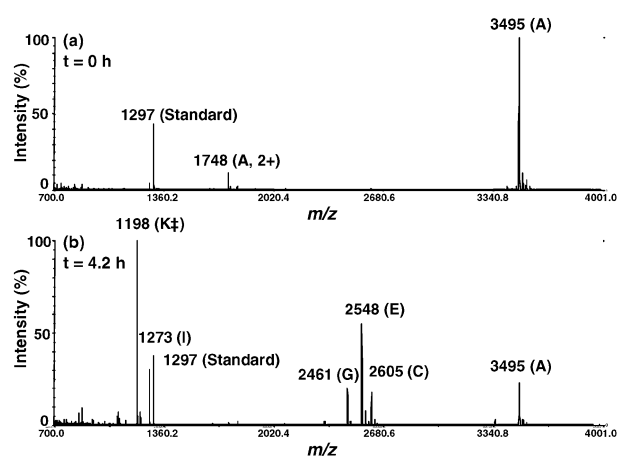


Fig. 3 Representative MALDI-TOF mass spectra for hydrolysis of 1 mM of insulin chain B at (a) *t* = 0 h and (b) *t* = 4.2 h. Reactions were run in 10 mM ZrCl₄ and 20 mM 4,13-diaza-18-crown-6 at pH 7.2 and 60 °C. Peak A is unhydrolyzed insulin chain B. Peaks K† and E and peaks I, G, and C correspond to apparent major and intermediate peptide hydrolysis products, respectively. Trace hydrolysis products are listed in Table S2 (in ESI). Human angiotensin I is the internal standard. All masses are singly charged unless otherwise indicated.

Gly-Glu was the most reactive of the 16 dipeptides studied.) The oxophilicity of Zr^{IV} combined with electrostatic interactions between this positively charged metal center and negatively charged $\text{Cys}(\text{SO}_3^-)$ could account for the efficient hydrolysis of the $\text{Cys}(\text{SO}_3\text{H})7\text{-Gly}8$ and $\text{Cys}(\text{SO}_3\text{H})19\text{-Gly}20$ amide bonds in bovine insulin chain B. In addition to the five major products, $\text{Zr}^{\text{IV}}/4,13\text{-diazia-18-crown-6}$ produced apparent intermediate amounts of hydrolysis at: $\text{Leu}6\text{-Cys}(\text{SO}_3\text{H})7$, $\text{Arg}22\text{-Gly}23$, and $\text{Gly}23\text{-Phe}24$. This pattern again may reflect the preference of Zr^{IV} for hydrolysis of peptides with glycine or oxygen-rich side chains. As shown in Fig. 1 and Tables S1 and S2 (in ESI), trace amounts of hydrolysis were seen at five sites within the oligopeptide.

Up until now, hydrolysis of oxidized insulin chain B has been studied using salts and/or complexes of Cu^{II} ,^{9b,g} Pd^{II} ,^{9b,c} Pt^{II} ,^{9g} and Zn^{II} .^{9h} These experiments were conducted under acidic conditions (pH 2.0 to 2.5) at temperatures ranging from 40 °C to 60 °C. Hydrolysis reactions were studied by ESI-MS,^{9b,g,h} HPLC-ESI-MS,^{9g} MS/MS,^{9g,h} and MALDI-TOF MS.^{9c} The data showed that metal binding sites included the *N*-terminal amino group of Phe1 (Cu^{II} , Pd^{II} , and Pt^{II}),^{9b,c,g} the imidazole side chains of His5 and His10 (Cu^{II} , Pd^{II} , Pt^{II} , and Zn^{II}),^{9b,c,g,h} and Arg22 (Zn^{II}).^{9h} If the metal-peptide complexes formed were hydrolytically active, then amide bond hydrolysis occurred in close proximity to the anchoring amino acid residue. Thus, the following insulin chain B peptide amide bonds were hydrolyzed: Phe1-Val2 (Cu^{II}),^{9g} Asn3-Gln4 (Cu^{II} , Pd^{II} , Zn^{II}),^{9c,g,h} His5-Leu6 (Zn^{II}),^{9h} Gly8-Ser9 (Cu^{II} , Pd^{II} , Zn^{II}),^{9c,g,h} His10-Leu11 (Pt^{II}),^{9g} and Glu21-Arg22 (Zn^{II}).^{9h} In urea-denatured oxidized hog insulin chain B, Pd^{II} produced cleavage at $\text{Leu}6\text{-Cys}(\text{SO}_3\text{H})7$ and at $\text{Gly}8\text{-Ser}9$.^{9b,10} Because no other cleavage sites were observed in any of the MS studies,^{9b,c,g,h} the hydrolysis of $\text{Cys}(\text{SO}_3\text{H})7\text{-Gly}8$ and $\text{Cys}(\text{SO}_3\text{H})19\text{-Gly}20$ amide bonds by $\text{Zr}^{\text{IV}}/4,13\text{-diazia-18-crown-6}$ points to unprecedented cleavage of insulin chain B at approximately neutral pH.

Metal salts of Ce^{III} , Ce^{IV} , La^{III} , Th^{IV} , and Zr^{IV} accelerate the lactamization of glutamate (Glu) to pyroglutamate (*pyro*Glu) at 70 °C over a weakly acidic to weakly alkaline pH range.¹¹ As shown in Fig. 2 and Fig. 3, Zr^{IV} -assisted hydrolysis of oxidized bovine insulin chain B produces peptide fragment K ($\text{Glu}21$ to $\text{Ala}30$, m/z 1216) and a second prominent peptide K^{\ddagger} (*pyro*Glu21 to $\text{Ala}30$, m/z 1198). We attributed the appearance of the latter fragment to loss of water through lactamization of the *N*-terminal glutamate residue in peptide K. Pyroglutamate formation was confirmed by ESI-MS/MS analyses of K^{\ddagger} , which produced a *pyro*Glu immonium ion at m/z 84.2. In addition to lactamization of glutamate, Ce^{III} , Ce^{IV} , La^{III} , Th^{IV} , and Zr^{IV} ions accelerate the hydrolytic deamidation of glutamine and asparagine residues.¹² In our experiments, HPLC-ESI analyses of the Zr^{IV} reactions detected the production of apparent trace quantities of the following three sets of insulin chain B peptides: $\text{B}^{\ddagger}(1)$ and $\text{B}^{\ddagger}(2)$; $\text{D}^{\ddagger}(1)$ and $\text{D}^{\ddagger}(2)$; and $\text{F}^{\ddagger}(1)$ and $\text{F}^{\ddagger}(2)$ (Table S1 in ESI). We then employed ESI-MS/MS sequencing to show that these fragments were produced by deamidation of parent peptides B, D, and F: in $\text{B}^{\ddagger}(1)$, $\text{D}^{\ddagger}(1)$, and $\text{F}^{\ddagger}(1)$, Gln4 in the corresponding parent was converted to Glu4; in $\text{B}^{\ddagger}(2)$, $\text{D}^{\ddagger}(2)$, and $\text{F}^{\ddagger}(2)$, Asn3 and Gln4 were deamidated to Asp3

and Glu4 (Fig. S4). Interestingly, deamidation of glutamyl and asparagyl residues occurs *in vivo*. Because a correlation exists between protein lifetime and total amide content, it has been suggested that deamidation may play a physiological role in triggering protein degradation.¹³

Up until now, the largest peptide to have been hydrolyzed by zirconium(iv) consisted of only four amino acid residues.¹⁷ We have successfully addressed this apparent limitation in the present study. By using HPLC-ESI-MS and MS/MS, and MALDI-TOF MS, we have demonstrated that $\text{Zr}^{\text{IV}}/4,13\text{-diazia-18-crown-6}$ facilitates hydrolysis of the 30-mer oligopeptide oxidized bovine insulin chain B at pH 7.0 and 60 °C. Apparent major levels of cleavage were produced at Gly8-Ser9, Gly20-Glu21, Ser9-His10, $\text{Cys}(\text{SO}_3\text{H})7\text{-Gly}8$ and $\text{Cys}(\text{SO}_3\text{H})19\text{-Gly}20$ sequences, while intermediate amounts of hydrolysis were at $\text{Leu}6\text{-Cys}(\text{SO}_3\text{H})7$, $\text{Arg}22\text{-Gly}23$, and $\text{Gly}23\text{-Phe}24$. $\text{Zr}^{\text{IV}}/4,13\text{-diazia-18-crown-6}$ was also shown to promote lactamization of *N*-terminal Glu21 and deamidation of Asn3 and Gln4. To the best of our knowledge, this paper presents the first example of metal-assisted hydrolysis of a $\text{Cys}(\text{SO}_3\text{H})\text{-Xaa}$ peptide amide bond. This is significant in light of the fact that the formation of cysteine sulfonic acid in proteins is triggered by oxidative stress and has been associated with amyloid fibril formation, Parkinson's disease, and physiological processes involving oxidative stress response proteins.¹⁴ Our current work is focused on mechanistic studies that should enable us to design new zirconium ligands that optimize sequence specificity and increase the hydrolytic efficiency of Zr^{IV} .

We thank the National Science Foundation for financial support under grant CHE-0718634.

Experimental

Peptide hydrolysis reactions

A total of 500 μM to 1 mM of oxidized bovine insulin chain B (freshly dissolved in doubly distilled H_2O) was added to 20 mM of 4,13-diazia-18-crown-6 in the presence or absence of 10 mM of ZrCl_4 (400 μL total volume). The pH value of the zirconium solution was adjusted at 25 °C to 6.9–7.2 by addition of the azacrown ether.⁷ (Alternatively, in the absence of ZrCl_4 , pH was adjusted with HCl.) Hydrolysis reactions were then allowed to proceed at 60 °C and aliquots were removed at $\sim t = 0$ h, 4 h, and 8 h time points. Pre- and post-reaction pH measurements varied by only ± 0.12 units. The aliquots were quenched at 4 °C with 1/10 volume of 0.5 M EDTA pH 8, and then analyzed by HPLC-ESI-MS or by MALDI-TOF MS. Each of the peptide fragments produced by $\text{Zr}^{\text{IV}}/4,13\text{-diazia-18-crown-6}$ was arbitrarily defined as either an apparent major, intermediate, or trace product depending on its percent relative abundance in the HPLC-ESI chromatograms recorded at $t = 4$ h or $t = 8$ h (Table S1 in ESI) and in MALDI-TOF mass spectra recorded at $t = 4.2$ h (Table S2): 44% to 100% for apparent major hydrolysis products, 12% to 30% for apparent intermediate hydrolysis products, 1% to 5% for apparent trace hydrolysis products.

Mass spectrometry

HPLC-ESI-MS and HPLC-ESI-MS/MS. HPLC-ESI chromatograms and corresponding mass spectra were acquired over a scanning mass range of m/z 100 to 3000 on a Micromass Q-ToF Micro mass spectrometer equipped with a Waters 2695 HPLC. Hydrolysis reactions were diluted 10-fold with doubly distilled H_2O . A 20 μL amount of each diluted solution was injected into a Waters AtlantisTM dC₁₈ 3 μm , 100 Å, 2.1 mm \times 150 mm reversed-phase HPLC column. Separations were conducted over 109 min at 20 °C with a flow rate of 0.2 mL min⁻¹ and a mobile phase gradient elution scheme consisting of 2% to 98% of acetonitrile in 0.1% formic acid. The ESI instrument settings were: electrospray needle voltage, +3.0 kV; N_2 cone gas flow, 60 L h⁻¹; N_2 desolvation gas flow, 450 L h⁻¹; capillary desolvation temperature, 200 °C. Spectra were acquired in positive ion mode (Fig. S1 to S4) or in negative ion mode (Fig. S5) with a scan time of 1.0 s.

HPLC-ESI-MS/MS sequencing of peptide fragments was done on the Micromass Q-ToF Micro mass spectrometer with data-directed acquisition (DDA). The MS to MS/MS switch criteria allowed a precursor selection of a maximum of 4 concurrent ions when the ion intensity was above a threshold of 10 ion counts per second. To induce collisional activation, the collision energy was set at 25 V and argon was used as a collision gas at a pressure of 28 psi.

MALDI-TOF MS. To prepare the CHCA matrix, a total of 10 mg of α -cyano-4-hydroxycinnamic acid was dissolved in 1 mL of water–acetonitrile (50 : 50, v/v) containing 0.1% trifluoroacetic acid. A total of 5 μL of the matrix was mixed with 5 μL of a ten-fold dilution of the peptide hydrolysis reaction and with 1 μL of an internal standard (1.5 μM human synthetic angiotensin I). A total of 1 μL of the resulting solution was transferred to a MALDI sample stage and air-dried. Positive ion MALDI-TOF mass spectra were then acquired using an Applied Biosystems Voyager-DE PRO Biospectrometry instrument in reflectron mode. Following time-delayed extraction, ions were accelerated to 20 kV. A total of 500 laser shots was averaged for each mass spectrum. The nitrogen laser source parameters included a grid voltage of 68.2%, a guide wire voltage of 0.001%, and a delay time of 50 ns. The average difference between calculated and observed mass values was $0.044 \pm 0.061 m/z$.

Software. All mass spectral peptide hydrolysis product peak assignments were made using FindPept software (The Swiss Institute of Bioinformatics; <http://ca.expasy.org/tools/findpept.html>). The majority of the peak assignments was subsequently confirmed by HPLC-ESI-MS/MS sequencing (Tables S1 and S2). Isotope distribution patterns were predicted using the “Isotope Distribution Calculator and Mass Spec Plotter” (Scientific Instrument Services, Inc.; <http://www2.sisweb.com/mstools/isotope.htm>). MS/MS fragmentation patterns were

predicted with MassLynx/BioLynx software, version 4.0 (Micromass).

References

- (a) K. W. Bentley and E. H. Creaser, *Biochem. J.*, 1973, **135**, 507; (b) W. Bal, J. Lukszo, K. Bialkowski and K. S. Kasprzak, *Chem. Res. Toxicol.*, 1998, **11**, 1014; (c) C. V. Kumar, A. Buranaprapuk, A. Cho and A. Chaudhari, *Chem. Commun.*, 2000, 597; (d) J. W. Jeon, S. J. Son, C. E. Yoo, I. S. Hong and J. Suh, *Bioorg. Med. Chem.*, 2003, **11**, 2901; (e) N. M. Milovic and N. M. Kostić, *J. Am. Chem. Soc.*, 2003, **125**, 781; (f) M. Kassai, R. G. Ravi, S. J. Shealy and K. B. Grant, *Inorg. Chem.*, 2004, **43**, 6130; (g) S. Manka, F. Becker, O. Hohage and W. S. Sheldrick, *J. Inorg. Biochem.*, 2004, **98**, 1947; (h) P. S. Chae, M.-S. Kim, C.-S. Jeung, S. D. Lee, H. Park, S. Lee and J. Suh, *J. Am. Chem. Soc.*, 2005, **127**, 2396; (i) A. Erxleben, *Inorg. Chem.*, 2005, **44**, 1082; (j) K. B. Grant and M. Kassai, *Curr. Org. Chem.*, 2006, **10**, 1035.
- (a) C. J. A. Wallace, in *Protein Engineering by Semisynthesis*, CRC, Boca Raton, Florida, 2000; (b) D. P. Humphreys, L. M. King, S. M. West, A. P. Chapman, M. Sehdev, M. W. Redden, D. J. Glover, B. J. Smith and P. E. Stephens, *Protein Eng.*, 2000, **13**, 201; (c) Q. Pan, W. Jiang, Z. Liao, T. Zhang and C. Liu, *Inorg. Chem.*, 2006, **45**, 490.
- R. C. Fay, in *Comprehensive Coordination Chemistry*, ed. G. Wilkinson, R. D. Gillard and J. A. McCleverty, Pergamon, Oxford, 1987, vol. 3, pp. 364.
- A. Singhal, L. M. Toth, J. S. Lin and K. Affholter, *J. Am. Chem. Soc.*, 1996, **118**, 11529.
- R. Smith and D. E. Hansen, *J. Am. Chem. Soc.*, 1998, **120**, 8910.
- M. Yashiro, T. Takarada, S. Miyama and M. Komiyama, *J. Chem. Soc., Chem. Commun.*, 1994, 1757.
- Because the pK_{a1} of 4,13-diaza-18-crown-6 is 7.94 at 25 °C, the azacrown ether was used to effectively buffer reaction pH^{1/}.
- V. C. Chen, K. Cheng, W. Ens, K. G. Standing, J. I. Nagy and H. Perreault, *Anal. Chem.*, 2004, **76**, 1189.
- (a) G. Allen and R. O. Campbell, *Int. J. Pept. Protein Res.*, 1996, **48**, 265; (b) X.-M. Luo, W.-J. He, Y. Zhang, Z.-J. Guo and L. Zhu, *Chin. J. Chem.*, 2000, **18**, 855; (c) N. M. Milovic and N. M. Kostić, *Inorg. Chem.*, 2002, **41**, 7053; (d) L. Zhu and N. M. Kostić, *Inorg. Chim. Acta*, 2002, **339**, 104; (e) L. Zhang, Y. Mei, Y. Zhang, S. Li, X. Sun and L. Zhu, *Inorg. Chem.*, 2003, **42**, 492; (f) S. H. Yoo, B. J. Lee, H. Kim and J. Suh, *J. Am. Chem. Soc.*, 2005, **127**, 9593; (g) J. Hong, R. Miao, C. Zhao, J. Jiang, H. Tang, Z. Guo and L. Zhu, *J. Mass Spectrom.*, 2006, **41**, 1061; (h) J. Jiang, Y.-H. Mei, W.-J. Wang, Q.-J. Wu and L. Zhu, *Wuji Huaxue Xuebao*, 2007, **23**, 948.
- Because no cleavage was observed when urea was omitted from this reaction,^{9b} it can be inferred that the interaction of oxidized insulin chain B with metals is dependent on protein secondary structure. Thus, in our experiments, the failure of oxophilic Zr^{IV} to produce hydrolysis adjacent to Glu13, Tyr27, and Thr28 may have been due to steric hindrance associated with secondary structure.
- E. Bamann and H. Muenstermann, *Arch. Pharm.*, 1965, **298**, 750.
- E. Bamann, H. Trapmann and H. Muenstermann, *Arch. Pharm.*, 1963, **296**, 47.
- (a) A. B. Robinson, *Proc. Natl. Acad. Sci. U. S. A.*, 1974, **71**, 885; (b) N. E. Robinson and A. B. Robinson, *Proc. Natl. Acad. Sci. U. S. A.*, 2001, **98**, 4367.
- (a) M. Chevallet, E. Wagner, S. Luche, A. van Dorsselaer, E. Leize-Wagner and T. Rabilloud, *J. Biol. Chem.*, 2003, **278**, 37146; (b) A. Lim, T. Prokaeva, M. E. McComb, L. H. Connors, M. Skinner and C. E. Costello, *Protein Sci.*, 2003, **12**, 1775; (c) T. Kinumi, J. Kimata, T. Taira, H. Ariga and E. Niki, *Biochem. Biophys. Res. Commun.*, 2004, **317**, 722.